

The BOND project: Biogenic aerosols and air quality in Athens and Marseille greater areas

R. E. P. Sotiropoulou, E. Tagaris, and C. Pilinis

Department of Environmental Studies, University of the Aegean, Mytilene, Greece

S. Andronopoulos, A. Sfetsos, and J. G. Bartzis

Environmental Research Laboratory, NCSR Demokritos, Attiki, Greece

Received 7 July 2003; revised 30 December 2003; accepted 19 January 2004; published 13 March 2004.

[1] The role of Secondary Biogenic Organic Aerosol in aerosol budget is examined using the Atmospheric Dispersion of Pollutants over Complex Terrain—Urban Airshed Model—Aerosols (ADREA-I/UAM-AERO) modeling system in two representative Mediterranean areas. The areas have been selected, because of their elevated biogenic emission levels and the sufficient degree of meteorological and land use diversity characterizing the locations. Comparison of the model results with and without biogenic emissions reveals the significant role biogenic emissions play in modulating ozone and aerosol concentrations. Biogenic emissions are predicted to affect the concentrations of organic aerosol constituents through the reactions of terpenes with O_3 , OH and NO_3 . The ozonolysis of terpenes is predicted to cause an increase in OH radical concentrations that ranges from 10% to 78% for Athens, and from 20% to 95% for Marseilles, depending on the location, compared to the predictions without biogenic emissions. The reactions of this extra hydroxyl radical with SO_2 and NO_x have as final products increased concentrations of sulfates and nitrates in the particulate phase. As a result, biogenic emissions are predicted to affect the concentrations not only of organic aerosols, but those of inorganic aerosols as well. Thus biogenic emissions should be taken into consideration when models for the prediction and enforcement of abatement strategies of atmospheric pollution are applied.

INDEX TERMS: 0345 Atmospheric Composition and Structure: Pollution—urban and regional (0305); 0317 Atmospheric Composition and Structure: Chemical kinetic and photochemical properties; 0305 Atmospheric Composition and Structure: Aerosols and particles (0345, 4801); *KEYWORDS:* aerosol models, biogenic emissions, secondary aerosols, Mediterranean, VOCs

Citation: Sotiropoulou, R. E. P., E. Tagaris, C. Pilinis, S. Andronopoulos, A. Sfetsos, and J. G. Bartzis (2004), The BOND project: Biogenic aerosols and air quality in Athens and Marseille greater areas, *J. Geophys. Res.*, *109*, D05205, doi:10.1029/2003JD003955.

1. Introduction

[2] Aerosols are a focus of attention, because of their important role in many areas, including human health, atmospheric reactions, acid deposition and the earth's radiation budget. For this reason, particulate matter is one of the thirteen pollutants covered by the European Council Directive on Air Quality Assessment and Management (96/62/EC).

[3] While progress has been made in understanding the direct input of particulate organic matter (primary sources), only scarce information is available today on the contribution of secondary organic aerosols (SOA). SOA are formed in the atmosphere by the mass transfer of low vapor pressure substances to the atmospheric particulate phase. First, a large parent organic is oxidized, giving products with vapor pressures significantly lower than that

of the parent. These products can partition between the gas and the aerosol phases via condensation and nucleation [Griffin *et al.*, 2002]. The condensable species are formed in the gas phase by the reaction of volatile organic compounds (VOCs) with the principal atmospheric oxidizing agents i.e., ozone, OH radicals and NO_3 radicals with various rates depending on the reactant [Atkinson, 2000]. Ozone is active during both daytime and nighttime hours. OH radicals are mainly produced during daylight hours from the photolysis of ozone while NO_3 is only active during nighttime hours as it photolyzes in the presence of sunlight [Jacobson *et al.*, 2000]. SOA can have anthropogenic (i.e., secondary anthropogenic organic aerosols) or biogenic origin (i.e., secondary biogenic organic aerosols). Biochemical processes that provide precursor materials for important aerosol species and the atmospheric processes that regulate the formation of these aerosols have been presented by Andreae and Crutzen [1997].

[4] Over 90% of the total VOCs entering the atmosphere are biogenic [Greenberg *et al.*, 1999]. Biogenic emissions of VOC from forests play an important role in regulating the atmospheric trace gas composition including global tropospheric ozone concentrations. Isoprene is ranked as the primary VOC emitted from trees in different locations [Isebrands *et al.*, 1999; Geron *et al.*, 2001, 2002], although experiments reveal forests where isoprene emissions are ranked second, exceeded by emissions of hexanol derivative compounds [Helmig *et al.*, 1999b]. The total flux of biogenic nonmethane volatile organic compounds (NMVOCs) in North America is found to be comprised primarily of isoprene (35%), 19 other terpenoid compounds (25%) and 17 nonterpenoid compounds (40%) [Guenther *et al.*, 2000]. Approximately 98% of the total annual natural NMVOCs emissions are emitted by vegetation. Natural emissions of NO, CO, and NMVOCs equal or exceed anthropogenic emissions on a global scale, although anthropogenic sources usually dominate within urban areas [Guenther *et al.*, 2000]. Many of the NMVOCs emitted from biogenic sources are highly reactive in the troposphere, with calculated lifetime of a few hours or less [Atkinson and Arey, 1998].

[5] Emission inventories are important in determining the flux of biogenic volatile organic compounds (BVOCs) into the atmosphere. Not only different kinds of vegetation emit different fractions of emitted BVOCs, but also the same kind of vegetation in different locations give different emission factors, due to differences in weather conditions and soil type. Flux potentials from different sites in US [Helmig *et al.*, 1999a, 1999b] reveal the necessity of emission inventories in each forest, in order to get more accurate result. The large number of terpenes, ~5000, including monoterpenes, sesquiterpenes, diterpenes and higher molecular weight species, which have been structurally determined, increase the difficulty in the construction of accurate emission inventories [Geron *et al.*, 2000]. The dominant emissions though are those of α -pinene, β -pinene, D3-carene, d-limonene, camphene, myrcene, β -phellandrene, sabinene, ocimene and p-cymene, depending on the forest site. In many areas α -pinene composes ~50% of the total monoterpene emissions [Geron *et al.*, 2000].

[6] Numerous gaseous and particulate products from the oxidation of biogenic organic compounds that have been investigated during the last couple of years reveal that the formation of secondary organic aerosol by ozonolysis of terpenes is very important [Yu *et al.*, 1999; Glasius *et al.*, 2000; Koch *et al.*, 2000]. On the basis of the nature and yield of various aerosol components, Yu *et al.* [1999] concluded that products such as pinic acid, pinonic acid, nonpinonic acid, hydroxy pinonic acid and hydroxy pinoaldehydes can act as molecular markers for secondary organic aerosol derived from biogenic sources. The formation of organic aerosols from the oxidation of biogenic hydrocarbons has been presented by Hoffmann *et al.* [1996, 1997]. The potential to form SOA is higher for cyclic parent hydrocarbons (α -pinene and d-3-carene) than for acyclic compounds (ocimene). Polyunsaturated biogenic alkenes (limonene) exhibit higher aerosol yield. For trans - caryophyllene, a natural emitted sesquiterpene, the aerosol yield is close to 1.0.

[7] The formation mechanisms of aerosol particles in a boreal forest site have been investigated by Kulmala *et al.* [2001], during the biogenic aerosol formation project (BIOFOR). The most probable formation mechanism was ternary nucleation which was followed by a growth into observable size before new particles appears. Jang and Kamens [1999] reported that the identification of carboxylic diacids, e.g., pinic acid, from α -pinene with ozone reaction provides important implication for the formation of self-nucleating biogenic aerosols.

[8] In addition to aerosol formation, biogenic emissions influence the ozone concentration. It has been reported by Poisson *et al.* [2001] that in an eucalyptus forest during daytime anthropogenic NMHC contribute between 10–15% whereas natural NMHC contribute between 5–25% to the observed O₃ levels. Moreover, isoprene chemistry reduces the OH radical concentration by a factor of two to three and contributes ~50–100% to the net ozone daytime photochemical production in this forested area. Modeling the effects of increased urban tree cover on ozone concentrations reveals that they generally reduce ozone concentrations in cities, but tend to increase average ozone concentrations in the overall modeling domain [Nowak *et al.*, 2000]. A model simulation for ozone formation in Atlanta revealed the significant role of natural hydrocarbons on it, although they comprised only a few percent of the total hydrocarbon burden [Chameides *et al.*, 1988]. As a result the effects of natural hydrocarbons must be considered in order to develop a reliable and effective strategy for controlling O₃. The role of anthropogenic and biogenic emissions on tropospheric ozone formation over Greece has also been simulated [Varinou *et al.*, 1999]. The simulations revealed that there was a significant increase of the calculated ozone concentrations over areas with significant precursor sources, when biogenic emissions are taken into account.

[9] In most Mediterranean countries, the burden of biogenic emissions is comparable with that from anthropogenic sources [Simpson *et al.*, 1999]. Besides the fact that the biogenic emissions govern the air chemistry and SOA formation in remote areas, biogenic sources have been documented to affect significantly air pollution in urban and near-urban environments. Cabada *et al.* [2002] have reported a strong dependency of the SOA contribution to the total organic PM concentration in Pittsburg, PA, varying from near zero during winter months to as much as 50% of the total OC concentrations in the summer.

[10] The role of biogenic emissions in aerosol formation has yet not been taken into consideration in European Air Quality legislation. A failure to do so, in particular in the Mediterranean region may result in ineffective control strategies, wasted expenditures and delays in reaching attainment of the targets. Air quality modeling supported by monitoring activities at the regions under consideration seems to be the only practical way today to cope with such a complex problem. Here, we examine the role of biogenic emissions in the aerosol budget, using the ADREA-I/UAM-AERO modeling system in two representative Mediterranean areas. The areas of the study have been selected because of the elevated biogenic emissions levels and the

sufficient degree of meteorological and land use diversity characterizing the locations.

2. Material and Methods

2.1. The Prognostic Meteorological Model

[11] The meteorological calculations have been performed using the ADREA-I model [Bartzis, 1989; Bartzis et al., 1991; Varvayannis et al., 1997]. The mesoscale prognostic model ADREA-I is a 3-D nonhydrostatic, fully compressible model, utilizing the conservation laws of mass, momentum, energy, humidity and in-ground heat conduction. The turbulence closure is obtained through a one-equation $k-l$ scheme. The model takes into account air/ground energy and mass interactions. ADREA-I utilizes a finite volume methodology for the numerical solution of the conservation equations, with a staggered grid for the velocities. It is fully implicit in time while it uses the upwind scheme for the convective terms. The SIMPLER/ADREA algorithm is adopted, which consists of transforming the mixture mass conservation equation into a full pressure equation, overall solution per time step by an iterative procedure, solution per variable by the Gauss-Seidel point iteration method and automatic time step selection based on convergence error bands. The equations are solved on a Cartesian, nonequidistant grid. The topography boundary surfaces are allowed to cross the computational cells (volume porosity and surface permeability concepts).

[12] The following boundary conditions were adopted in the present case: at the domain top plain the vertical velocity component, the turbulent kinetic energy, and the vertical fluxes of the horizontal wind components as well as of the specific humidity were all set to zero. At the northern and western boundaries, the profiles of the horizontal wind components were fixed at their initial values. At the southern and eastern boundaries, the horizontal fluxes of the horizontal wind components were assumed to be zero. At all lateral boundaries, the horizontal fluxes of all the other solved parameters were set equal to zero. At zero height above ground level all the velocity components and the turbulent kinetic energy were set to zero. These boundary conditions were kept constant throughout the simulation period in order to eliminate the effects of inaccuracies in the initial wind velocity and temperature fields. The ground surface temperature has been calculated through the one-dimensional ground heat budget equation. The sea surface temperature is assumed constant at 18°C.

2.2. The Three-Dimensional Photochemical Modeling Tool

[13] The UAM-AERO model [Sonoma Technology, Inc., 1996] is a gas/aerosol model that is based on the air quality model UAM version IV (UAM-IV) [System Applications International (SAI), 1990a, 1990b, 1990c, 1990d, 1990e]. The procedures used in the UAM-AERO model to simulate gas-phase chemical reactions and dry deposition of gases are similar to those in the UAM-IV with the following modifications: (i) Gas-phase chemistry is replaced by a more flexible interface that allows the chemical mechanism to be easily changed [Kumar et al., 1995]. For this simulation UAM-AERO was used with the SAPRC90 [Carter, 1990] chemical mechanism (ii) Integration of

gas-phase kinetics is done by using the high accuracy LSODE solver [Hindmarsh, 1983], (iii) Production of sulfuric acid from aqueous phase oxidation of sulfur dioxide, (iv) Condensable organics are produced using the yields reported by Pandis et al. [1992], (v) The gas-phase chemical kinetic rate expressions are calculated from 3-dimensional temperature and water vapor concentration fields, and, (vi) dry deposition is calculated using an algorithm based on Wesely [1989].

[14] The SAPRC90 chemical mechanism is comprised of fifty chemical species (eleven fast reacting; thirty slow reacting; seven steady state and two constant species, CH₄, H₂O), solar radiation and one hundred thirty chemical reactions. Primary emissions of organic compounds are assigned to nine lumped classes. Among the lumped classes there are two categories of alkanes (less reactive with $\text{kOH} \leq 10,000 \text{ ppm}^{-1}\text{min}^{-1}$ (ALK1), more reactive with $\text{kOH} > 10,000 \text{ ppm}^{-1}\text{min}^{-1}$ (ALK2)), four categories of olefins (less reactive with $\text{kOH} \leq 75,000 \text{ ppm}^{-1}\text{min}^{-1}$ (OLE1), more reactive with $\text{kOH} > 75,000 \text{ ppm}^{-1}\text{min}^{-1}$ (OLE2), isoprene (OLE3), terpenes (OLE4)), two categories of aromatic compounds (less reactive with $\text{kOH} \leq 20,000 \text{ ppm}^{-1}\text{min}^{-1}$ (ARO1), more reactive with $\text{kOH} > 20,000 \text{ ppm}^{-1}\text{min}^{-1}$ (ARO2)) and three categories of aldehydes (formaldehyde (HCHO), acetaldehyde (CCHO), propionaldehyde and higher aldehydes (RCHO)). The specific mechanism is also designed to simulate the production of condensable organic species from the oxidation of higher molecular weight gaseous VOCs.

[15] The aerosol size distribution treatment in the model is based on a fractional representation with user-applied size bins. The number of size sections used depends on the accuracy level desired. The simulation of the aerosols-size distribution is necessary for the accurate simulation of the chemical evolution of the aerosol and the aerosol removal by deposition. The larger the number of size bins is, the more accurate the results are. However, the use of a large number of size – sections increases the CPU requirements of the simulation. Thus a typical number of 4 to 8 size sections from 0.01 to 10 μm for aerosols and one or more size sections from 0.01 to 30 μm when fog droplets are present are used. Simulation of the aerosol concentrations of all primary and secondary components of atmospheric particulate matter includes sulfate, nitrate, ammonium, chloride, sodium, elemental carbon, organic carbon, water and other crustal materials. The default geometric mass mean diameters proposed by UAM-AERO [Sonoma Technology, Inc., 1996] were used for the aerosol species. In particular, the mean diameters used were 1.3 μm for SO_4^- , 1.2 μm for NO_3^- , 1.1 μm for NH_4^+ , 2.4 μm for Na^+ , 1.7 μm for Cl^- , 1.8 μm for OC, 1.6 μm for EC, 2.1 μm for OTR, 1.5 μm for H₂O and 1.6 μm for H⁺ under nonfog conditions, while under fog conditions the mean diameters are doubled. The aerosol model is based on the assumption of internally mixed aerosol; this implies that all particles in a size section are assumed to have the same chemical composition. The physical processes considered are: advection, turbulent diffusion, condensation and evaporation coagulation, emissions, nucleation and deposition. The effect of the presence of fog on gas and aerosol species is simulated in an empirical manner. Particle growth and shrinkage are determined by the amount of water transferred to and from

particles, based on equilibrium concentrations estimated by ISORROPIA [Nenes *et al.*, 1998, 1999] which calculates the equilibrium of 26 species (4 gas phase, 13 liquid phase and 9 solid phase) and has been chosen for its computational efficiency and comprehensive treatment of aerosols.

2.3. Interface Between Meteorological and Photochemical-Aerosol Model

[16] The 3-dimensional wind fields calculated by the meteorological model were archived on an hourly basis to be used as input by the photochemistry model. The computational grids used in the meteorological and photochemistry models are different, both horizontally and vertically. The meteorological model grid is Cartesian whereas the UAM grid is terrain-following, variable in space and time. Therefore in order to ensure the conservation of mass, the wind field produced by the meteorological model is passed through a diagnostic wind model, which is a pre-processor of the UAM-IV [SAI, 1990c]. Thus a mass-consistent wind field is obtained for the ten UAM layers. Other calculated meteorological variables used as input in the photochemistry-aerosol model are the near-ground air temperature, the mixing layer height, the temperature gradients below and above the mixing layer height and the humidity.

[17] Additional data used were the topography, the land cover, the anthropogenic and biogenic emission inventories, covering the Greater Athens Area (GAA) in Greece and the Greater Marseilles Area (GMA) at the south coast of France. These two sites were selected as representative Mediterranean areas with intense air pollution activity.

2.4. Description of the Greater Athens Area

[18] The cities of Athens, Piraeus and their suburbs constitute the Athens basin. The basin is surrounded by the mountains of Hymettus to the E, Pendeli to the N-NNNE and Parnitha to the N-NNW with elevation up to 1400 m while to the south is defined by the coast. The length of the basin is ~ 25 Km (with direction from SSW to NNE) and the width is ~ 17 Km. The basin's declination is $< 1\%$ at the slopes of the mountains. The mountains mentioned above are the physical barriers between the Athens Basin and the plains of Thriassion and Mesogea. Between those mountains there are three big physical gaps. In the Athens Basin there are also three hills, with elevation up to 150 m above the bottom of the basin. The main urban mass (~ 4 million inhabitants) is concentrated in the Athens Basin. The geographic expansion of the area not followed by the parallel development of the necessary infrastructures (road network, parks etc.) causes increasing problems of pollution all over the basin for the last 40 years.

[19] The main sources of air pollution in the Greater Athens Area (GAA) can be classified into three main categories: a) industry ($\approx 40\%$ of the total Greek industrial activity), b) transportation ($\approx 50\%$ of the total automobile traffic) and c) heating. The main source of photochemical pollutants is considered to be transportation. The harbor of Piraeus, the biggest in the country and the international airport of Athens are also considered important sources of air pollution. Most of the industrial activities in the GAA and the country are concentrated in and west of the Thriassion Plain.

[20] The dimensions of the modeling domain for the GAA were selected on the basis to include the Athens urban area, containing the bulk of the anthropogenic emissions, as well as an extended surrounding rural area with biogenic emissions. It extends from 93 km west to 91 km east and from 91 km south to 93 km north of the city of Athens, covering a total area of 33856 km². The domain on which UAM-AERO was applied was a 92×92 grid system, with horizontal grid increments of 2 km in both directions (Figure 1a). The center of the domain was the National Observatory of Athens ($37^\circ, 58'$; $23^\circ, 43'$). In the vertical, 10 layers of variable thickness were used, up to 3000 m above ground level, 7 under and 3 above the diffusion break, for both episodes. The domain was chosen in such way that the boundary concentrations could be assumed to be background concentrations, compared to the concentrations in the basin. Data from the literature were used as initial conditions for 24 gas species and eight aerosol constituents. The distribution of these aerosol species to the different size sections was made, following the assumption that aerosols follow a lognormal distribution. The default geometric mass mean diameters proposed by UAM-AERO [Sonoma Technology, Inc., 1996], as described above, were used for the aerosol species. Moreover, a geometric standard deviation of 2.0 was used for all aerosol classes.

[21] Gridded hourly anthropogenic emissions have been estimated, based on traffic information and the industrial activities in the domain. Biogenic emissions of NO, isoprene and terpenes at ground level were constructed, based on the Biogenic Emission Inventory System (BEIS) [Pierce *et al.*, 1990]. In order to estimate ammonia emissions over the entire area, primary data concerning the animals, the types of cultivations and the areas covered by them were obtained from the National Statistical Service of Greece as these are the three main categories that are responsible for the ammonia emissions in the GAA [Sotiropoulou *et al.*, 2004].

2.5. Description of the Greater Marseilles Area

[22] Marseille is located in the Rhone Delta at the south end of the Rhone Valley, a long north-south rift between the Cevennes Mountains and the foothills of the French Alps. A 955 m rounded summit is located ~ 26 km northeast of Marseille and a 720 m summit is located ~ 11 km northeast of the port. Other summits east of Marseille may also be seen. The sea shore area is divided into two small basins: a first one including the one million inhabitant city of Marseille surrounded by mountains with summits ranged between 500 and 1000 m. A second one located 15 km NW of Marseille is characteristic of a strong industrial zone. Natural lands are covered with agricultural activities as well as with Mediterranean vegetation. The Gulf of Marseille is bordered by the French landmass from northwest clockwise through southeast. Owing to the topography of the region, however, it is only partially shielded from the effects of winds emanating from the eastern semicircle. Smog episodes occur generally during sea breeze time. These pollution events are a mixture of aged and newly formed smog of urban and industrial emissions, as well as strong biogenic and anthropogenic emissions. The city of Toulon lay on the southeast border of the domain.

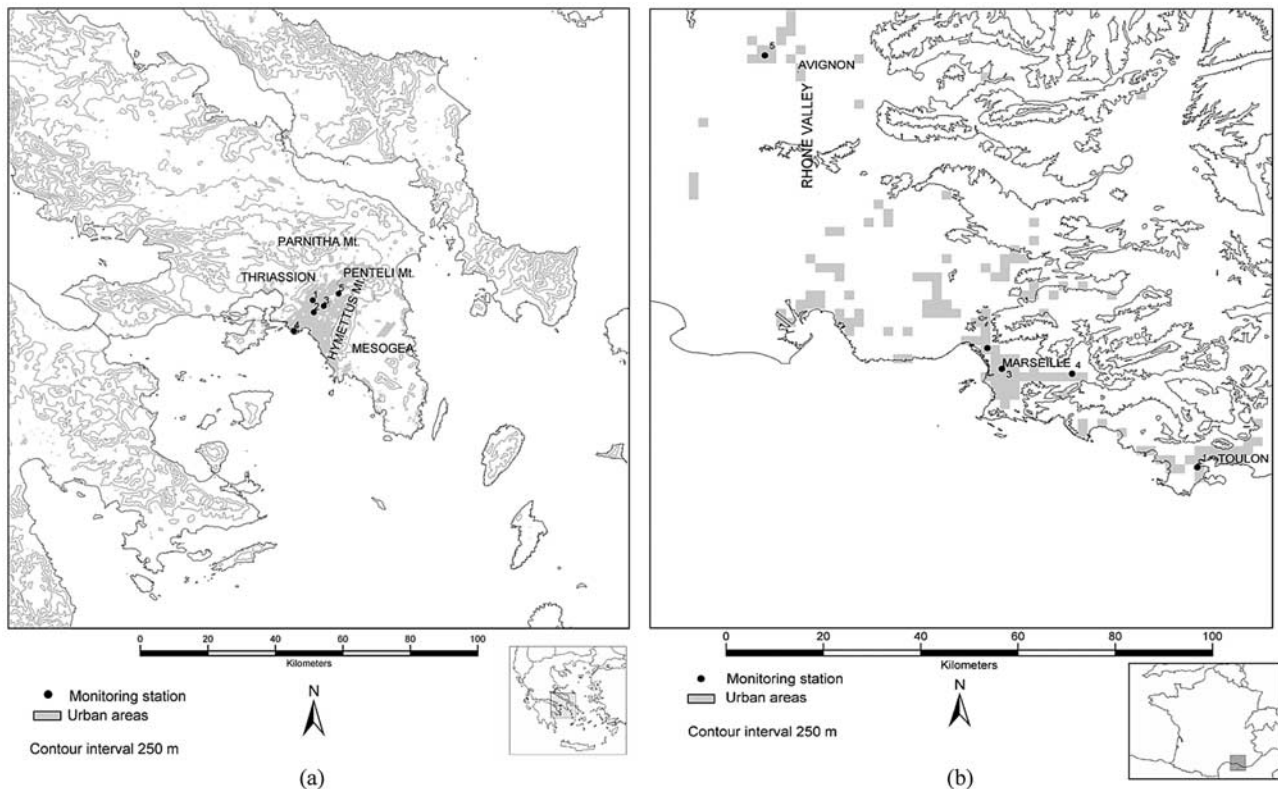


Figure 1. (a) Greater Athens Area (GAA) modeling domain. (b) Greater Marseilles Area (GMA) modeling domain.

[23] The GMA domain was selected by taking into account the geographic extension of the available topographical, land cover, anthropogenic and biogenic emission data. It extends from 71 km west to 57 km east and from 57 km south to 79 km north of the city of Marseille and it covers an area of 17408 km². The domain on which UAM-AERO was applied was a 64 × 68 grid system, with horizontal grid increments of 2 km in both directions (Figure 1b). In the vertical, 10 layers of variable thickness were used, up to 5500 m above ground level, 6 under and 4 above the diffusion break, for all days. As in the case of the GAA, data from the literature were used as initial conditions for 24 gas species and eight aerosol constituents. The distribution of these aerosol species to the different size sections was made, following the assumption that aerosols follow a lognormal distribution using the default geometric mass mean diameters proposed by UAM-AERO [Sonoma Technology, Inc., 1996] and a geometric standard deviation of 2.0 in all classes.

[24] In addition, gridded hourly anthropogenic, as well as biogenic emissions were used. These data were provided to us by the University of Louis Pasteur, France in the framework of the European Research Project Biogenic Aerosols and Air Quality in the Mediterranean Area (BOND).

3. Results and Discussion

[25] Two episodes were selected, one for Athens and one for Marseilles. For each episode two simulations were performed, a base case simulation without biogenic emis-

sions and a second with biogenic emissions, using the meteorological data of the episodic day, as predicted by ANDREA I. In this way we can examine the effects of the inclusion of biogenic emissions on the concentrations of gaseous and particulate compounds of interest.

3.1. Application of the Modeling System in the Greater Athens Area: The Episode of 25 May 1990

[26] The episode of May 25, 1990 was characterized by favourable conditions for the accumulation of primary and secondary pollutants over the Athens basin: weak synoptic wind, sea-breeze development and stable temperature stratification [Pilinis *et al.*, 1993; Andronopoulos *et al.*, 1998; Sotiropoulou and Pilinis, 2001]. During this episode, the synoptic flow during the night and until sunrise was from NW in the lower layers with no significant changes aloft (Figure 2a). Only after 1100 (LST), a light (for this season) sea breeze of S to SW direction ($2\text{--}4\text{ ms}^{-1}$) started to develop with three main systems in the Attica peninsula: over the eastern Mesogea plain, in the Athens central basin and over the western Thriassion plain (Figure 2b). There are convergence zones where the opposing sea breezes meet: at the northeast of the central basin (between the mountains Parnitha and Penteli), at the east (between the mountains Penteli and Hymettus) and at the south-east (between Hymettus and the southern topography). There appears to be a balance between the sea breezes that meet at the convergence zones. Thus the flow out of the Athens basin through the mountains gaps is blocked and this increases the air pollution levels in the city. Wind divergence phenomena also occurred over Peloponnesse, as indicated by Kotroni *et*

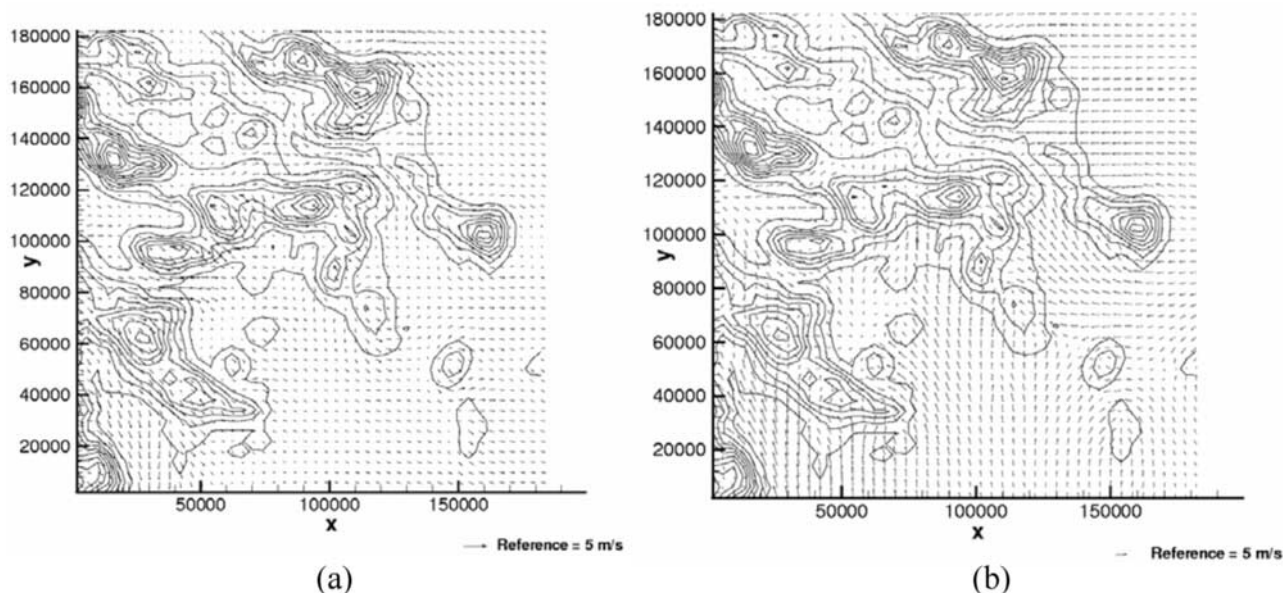


Figure 2. Wind fields ~ 10 m above ground level for the GAA episode of May 25, 1990 at (a) 0600 LST and (b) 1600 LST.

al. [1999]. The atmosphere over the GAA was very stable, and the vertical mixing height, ranged between 150 to 200 m during the afternoon and 60 to 100 m during the night.

[27] In order to avoid any domination by the initial conditions onto the predictions, multiple repeat runs were performed, to wash out errors in the initial conditions. As predicted by the model, there is strong influence of the initial conditions during the first run, which decreases during the first repetition, while there is stabilization during the next three repeated runs. Thus a spin up time of four days was used to wash out errors in the initial conditions and to emphasize the physics and chemistry simulated in the model.

[28] The predicted spatial distribution of the concentrations of ozone and secondary anthropogenic SO_4^- , NO_3^- , NH_4^+ , OC, as well as their increase when biogenic emissions are considered, are presented in Figures 3a and 3b respectively. Their spatial distributions reveal higher concentrations in the suburbs north of the Athens city-center. The sulfate distribution shows one maximum concentration, due to the SO_2 emitted from the Thriassion industrial area and transported N-NE, due to the prevailing winds. This is supported by the windfield shown in Figure 2b. The nitrate distribution, on the other hand, depicts two maxima, one at the same location with the sulfate peak, which is due to the HNO_3 produced from NO_x of industrial origin, and a second peak S-SE of the first, which is due to the HNO_3 produced from NO_x emitted from cars and other vehicles in downtown Athens.

[29] The profile of the spatial distribution of NH_4^+ concentrations is a combination of the spatial distributions of SO_4^- and NO_3^- , as NH_3 is the only basic component in our model. Finally, the spatial distribution of the secondary anthropogenic OC, the only organic aerosol constituent in our model, indicates the high emissions of its precursors, such as alkanes, alkenes and aromatics, at that part of the domain.

[30] The spatial distribution of the increase of ozone and aerosol concentrations, as a result of the inclusion of biogenic emissions, indicates that, not only the concentrations of OC are affected, but also the concentrations of both ozone and inorganic aerosol species. As shown in Figure 3, a moderate increase is predicted in the concentrations of aerosol species and ozone in the city of Athens and its suburbs, while a higher increase is predicted in the rural areas where the biogenic emissions are placed. Owing to the calm winds, biogenic gasses remain in the rural areas and react with ozone.

[31] The increased concentration of OC is due to the production of condensable organic compounds from the reaction of terpenes with O_3 , OH and NO_3 . The increased ozone concentrations, when biogenic gasses are considered, are due to the reaction of biogenic hydrocarbons with NO_x . Moreover, the ozonolysis of terpenes is a significant source of OH radicals in the troposphere [Pfeiffer *et al.*, 1998]. From the ozonolysis of biogenic compounds the produced OH reacts with SO_2 and NO_x , leading to the formation of inorganic aerosol species. It is worth mentioning that UAM-AERO predicts an increase of OH that ranges from 10% to 78%, depending on the location, when biogenic emissions are considered, compared to the application of the model without biogenic emissions. In order to verify the origin of these OH radicals in UAM-AERO, we repeated the application of the model, leaving out the ozonolysis of terpenes. The increase of OH production was only up to 12.9%, depending on the location, when biogenic emissions are considered, which indicates that the increase of OH is mainly caused by the ozonolysis of terpenes.

[32] Measured and predicted time series concentrations of O_3 , NO and NO_2 at five monitoring stations, as well as the corresponding increase of the concentrations, as a result of the inclusion of biogenic emissions, are presented in Figure 4. As shown in the figure, the model simulated the ozone diurnal pattern reasonably well. The

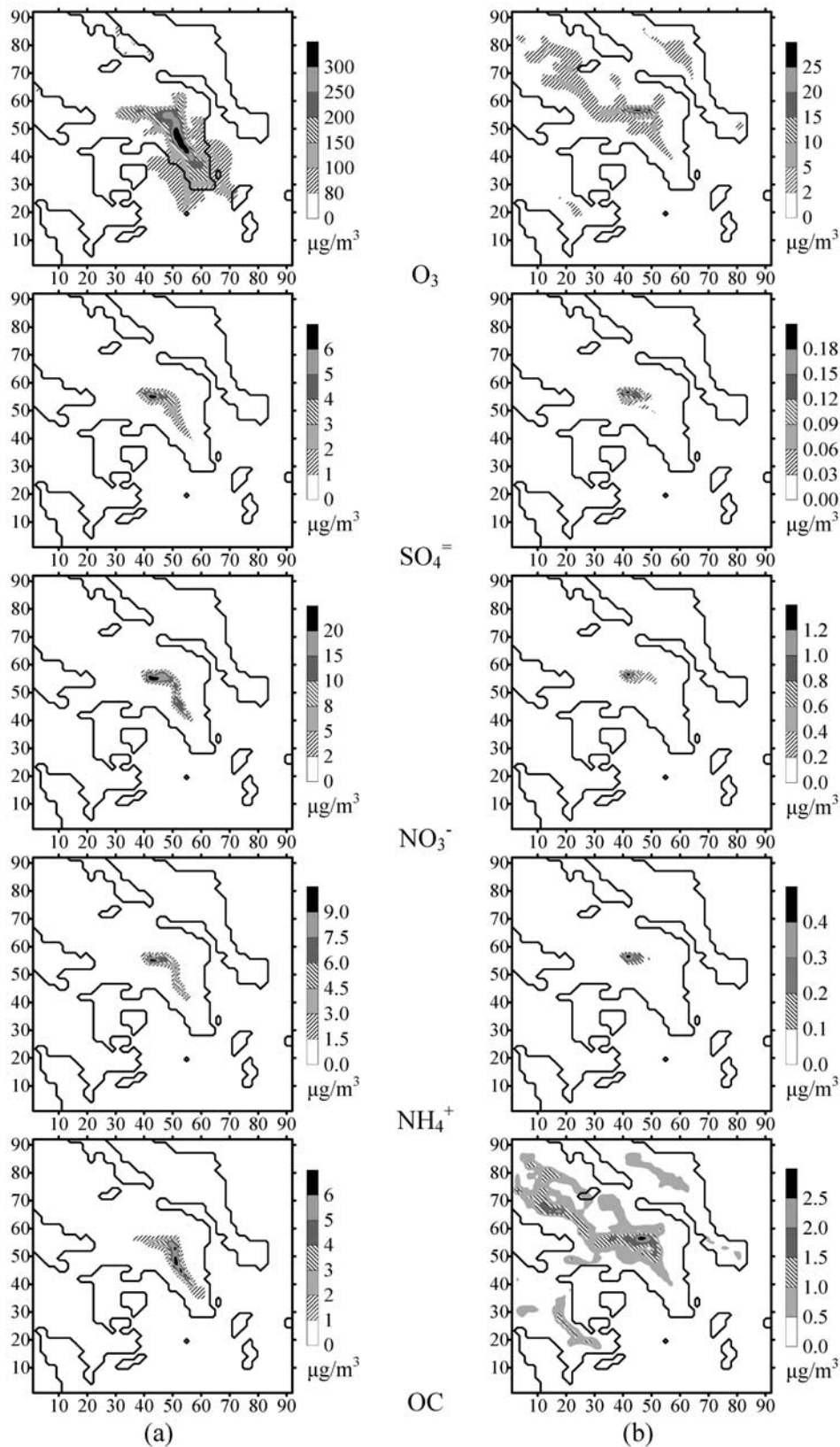


Figure 3. Spatial distributions of (a) predicted ground level concentrations in the GAA at 1500 LST when no biogenic emissions are used and (b) predicted increase in the corresponding concentrations when biogenic emissions are included. See color version of this figure in the HTML.

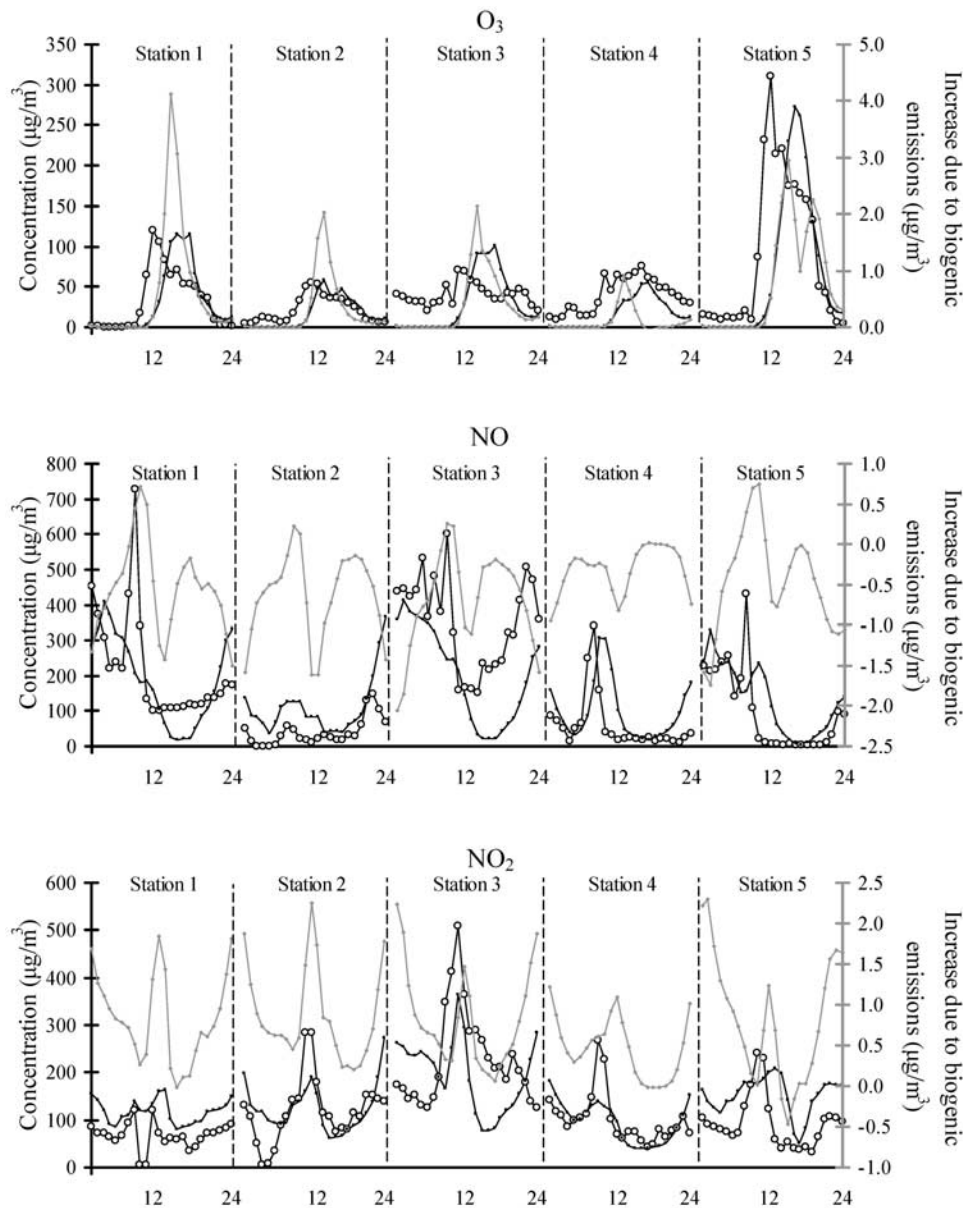


Figure 4. Predicted (squares) and observed (circles) time series concentrations (left y-axes) and increase (diamonds) due to biogenic emissions (right y-axes) for five monitoring stations in the GAA. See color version of this figure in the HTML.

low values of ozone during the night, when no photochemical reactions take place, are clearly depicted. The daytime maximum ozone concentration is higher than the observed at two of the sites and lower at the others, while at all sites there is a delay in the appearance of the maximum, caused either by inaccuracies in the emission inventory or by the radiation factor provided by the meteorological model. One though, must be cautious when he compares predicted and measured values, since the observed values are at a fixed point, whereas the model concentrations refer to the average value for each grid. The influence of biogenic emissions on the ozone concentrations in the city of Athens seems to be small, increasing ozone concentrations, only up to 5% in the city center, compared to the simulation for which biogenic emissions are not included.

[33] The performance of the model for NO and NO_2 is also good, as there is agreement between the measured and the predicted concentrations in all stations, although the model fails to predict the sudden peaks.

[34] The predicted secondary anthropogenic SO_4^{2-} , NO_3^- , NH_4^+ , OC concentrations at two representative urban monitoring stations, as well as the predicted increase due to the presence of biogenic gasses are presented in Figure 5. During the morning hours the model predicts a significant production of secondary inorganic aerosols. This is the result of the increased water content of the atmosphere due to high relative humidity ($\sim 90\%$ at 0200 LST at the Hellinikon meteorological station), which favors the formation of aqueous solution of SO_4^{2-} , NO_3^- , NH_4^+ . After midday the water content of the atmosphere decreases (the relative humidity was $\sim 50\%$ at 1400 LST at the Hellinikon station),

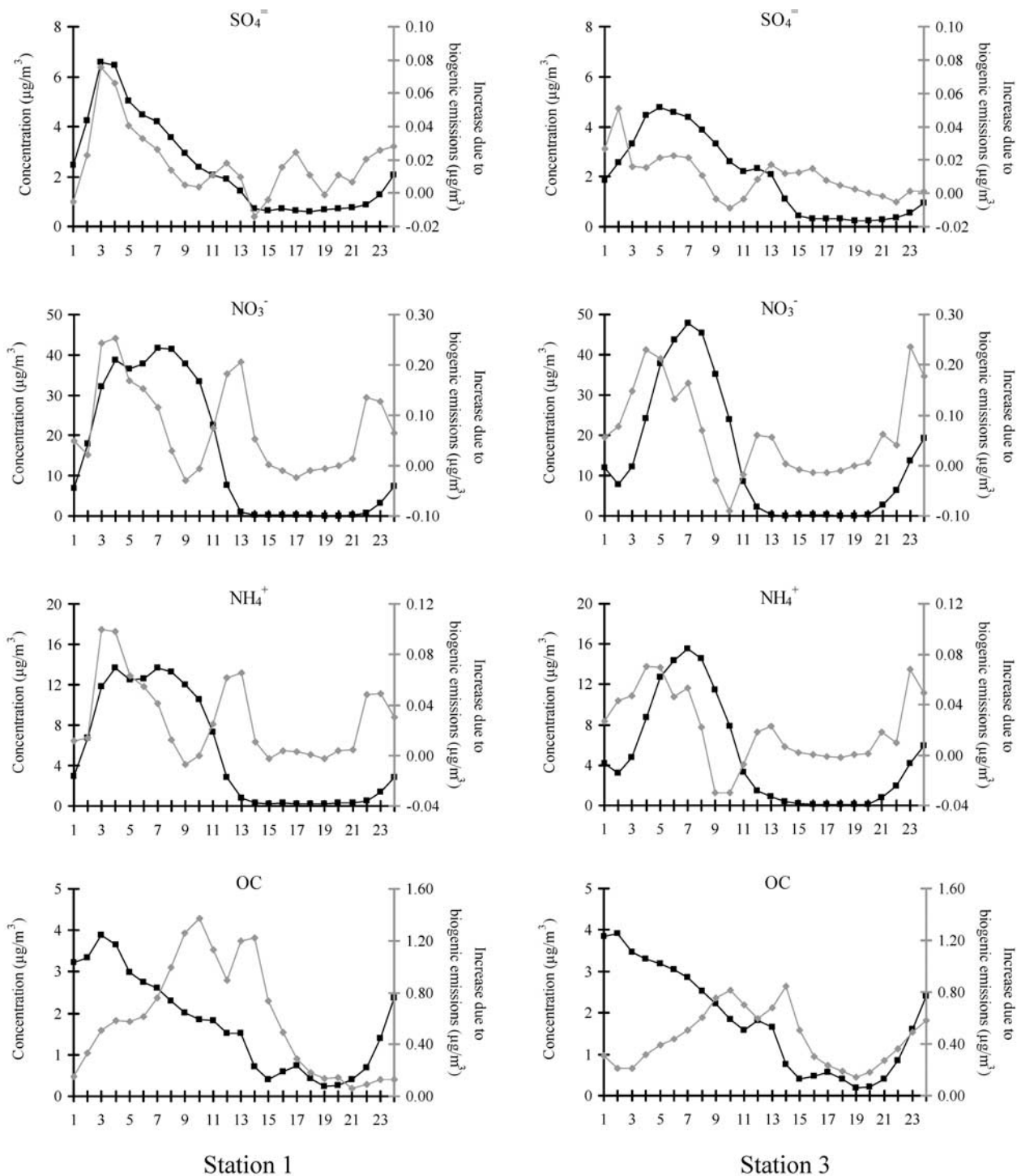


Figure 5. Predicted (squares) time series concentrations (left y-axes) and increase (diamonds) due to biogenic emissions (right y-axes) for two monitoring stations in the GAA.

due to the high temperature, and as a result, smaller quantities of NH_3 , H_2SO_4 and HNO_3 are dissolved, or form solid inorganic salts. This, in combination with both the dry deposition of aerosols and the direction of the wind field that drives the pollutants out of the city center, cause the reduction of their concentrations. The time series of NH_4^+ concentrations follows that of NO_3^- . Nitrate is the most abundant ionic compound during the morning hours in the

stations presented, indicative of the strong production of nitric acid in the city center, due to the increased traffic volume. Sulfate on the other hand is less important, due to absence of industrial activities, responsible for the SO_2 emissions, at that part of the domain.

[35] The aerosol concentrations change when biogenic emissions are considered. This change is more profound after midday, when the biogenic production is higher.

Although there are insignificant biogenic emissions in the city of Athens, where the presenting monitoring stations are sited, their contribution in the aerosol budget is very important for OC and less important for the inorganic aerosols. OC is quickly formed from condensable organic compounds, produced by the reaction of terpenes with gaseous NO_3 , OH radicals and O_3 . The ozonolysis of terpenes leads to the formation of OH and HO_2 radicals, which in turn react with SO_2 and NO_x forming H_2SO_4 and HNO_3 respectively.

[36] During the afternoon hours an increase in the aerosol deposition rates is predicted, due to the accumulation of the mass in the bigger size-bins, which is caused by the higher condensation rate of condensable compounds, due to an increase of their concentrations. This results in an increased gravitational deposition of the aerosol species. Comparing the deposition with and without biogenic emissions one observes higher deposition rates when biogenic emissions are considered. For the Station 1, in particular, an increase of the deposition rate up to 60% for OC, 80% for SO_4^- and 10% for NO_3^- is predicted, while for the Station 2 the percentages are 40, 60 and 35 per cent, respectively. The production rate of OC by reactions of biogenic organic gases is higher than the quantity deposited in both stations, leading to an increase in the predicted values. Regarding sulfates, for the same time period, its production exceeds the deposited quantity in the first station leading to a net increase of almost 6%, in contrast to the second stations, where the deposition is higher.

[37] In both monitoring stations the predicted NO_3^- concentrations are decreased due to the dry deposition that exceeds the produced quantities. This behavior explains also the predicted NH_4^+ concentrations at night, which follow those of NO_3^- . The modeling results showed that the maximum impact on ozone and aerosol concentrations, due to biogenic emissions, does not coincide in time with their maximum concentrations. So, the maximum concentrations are less affected, and it is rather the rate at which ozone and aerosol concentrations increase or decrease that is altered. *Thunis and Cuvelier* [2000] reported the same result regarding the influence of biogenic emissions on O_3 concentrations.

3.2. Application of the Modeling System in the Greater Marseilles Area: The Episode of 29–30 June 2000

[38] The GMA episode between June 29, and June 30, 2000 was characterized by strong north-westerly flow in the first day and the formation of sea-breeze during the second day. Data were available through the mesoscale model inter-comparison exercise, related to the ESCOMPTE pre-campaign, organized and conducted by French institutions in the summer of 2000 (available at <http://medias.obs-mip.fr/escompte>). Temperature and wind measurements are also available for 56 stations in the domain of interest on an hourly basis, although not every station had all the variables available. Figure 6 presents the predicted wind fields on 0600 and 1600 LST for both days. Owing to topographic effects, the wind speed was lower on the top right part of the domain that is predominantly open fields.

[39] As in the case of the GAA, in order to avoid any domination of the initial conditions onto the predictions, multiple repeated runs were performed. As predicted by the

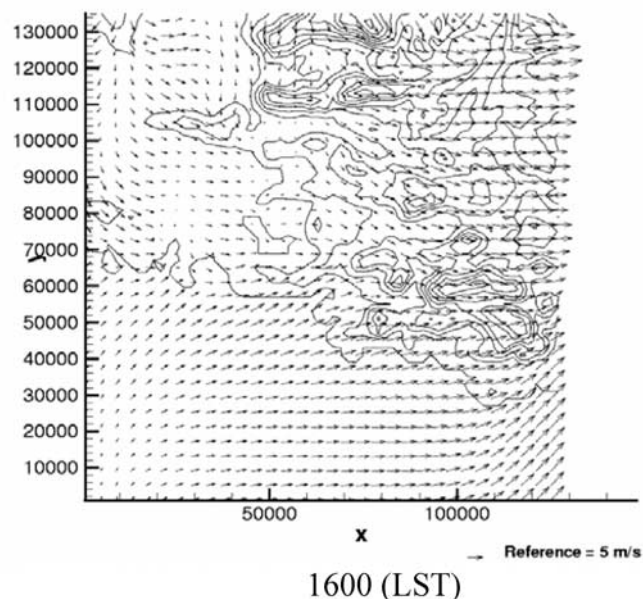
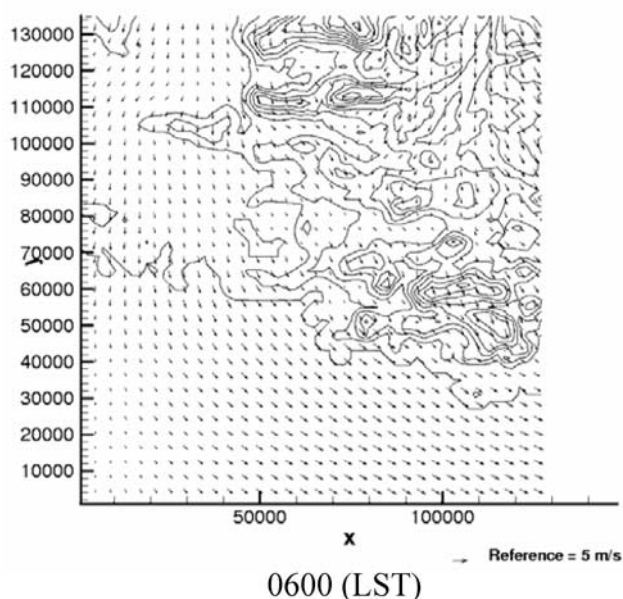
model, there is influence of the initial conditions during the first run while there is stabilization during the next three runs. Thus a spin up time of three days was used.

[40] The predicted spatial distribution of the concentrations of ozone and secondary anthropogenic SO_4^- , NO_3^- , NH_4^+ , OC, as well as their increase when biogenic emissions are considered, are presented in Figures 7a and 7b, respectively. These spatial distributions reveal higher concentrations at the north suburbs of Marseille and Toulon. The profiles of the spatial distributions of SO_4^- , NH_4^+ and O_3 are similar, due to the increased photochemical activity at that part of the domain. Higher NO_3^- concentrations are noted in areas with low SO_4^- concentrations. Owing to the low volatility of H_2SO_4 , compared to the volatility of HNO_3 , H_2SO_4 quickly forms SO_4^- in the presence of basic components, such as NH_3 , while HNO_3 tends to remain in the gas-phase, until NH_3 concentrations reach high enough levels to cause the formation of nitrates. OC is almost uniformly distributed throughout the domain due to the low concentrations of anthropogenic organic aerosol precursors. The concentrations of alkanes, mainly those with more than 6 C-atoms [*Grosjean and Seinfeld*, 1989] and aromatic species, which are considered as the most important species in the formation of condensable organics, in the absence of biogenic compounds, are 200% and 25% lower in GMA than in the GAA, respectively. The uniform background concentrations, in combination with the strong wind field that drives the pollutants out of the domain lead to the predicted small spatial variation of the OC concentrations.

[41] The change in the inorganic aerosol concentrations, when biogenic gasses are considered shows higher increase from the center of the domain to the southeastern part of it. This is due to the strong winds which transport biogenic gasses at that part of the domain, where they react with ozone, producing OH. Application of the model with biogenic emissions reveals 20% to 95% higher concentrations of OH, compared to application of the model without biogenic emissions. OH, in turn, reacts with SO_2 and NO_x , giving aerosol species. The increased concentration of OC is due to the production of condensable organic compounds from terpenes, which in turn give OC. The increased ozone concentrations are caused by the reaction of hydrocarbons with NO_x .

[42] In order to validate model's performance for the GMA, the predicted and observed time series O_3 , NO and NO_2 concentrations, as well as the increase due to biogenic emissions for five representative monitoring stations are presented in Figure 8. The model exhibits a reasonable behavior, for all monitoring stations. The influence of biogenic emissions to ozone concentration levels seems to be more important for the city of Marseille than it is for Athens. Although there are unimportant local biogenic emissions in the city of Marseilles, the predicted ozone concentrations, when biogenic emissions are considered, increase up to 25% for the days of the simulation. This is due to the prevailing winds, which drive the high concentrations of precursors of biogenic origin over the cities of Marseilles and Toulon. As pollutant sources are placed near the coast, sea breeze transports them in the mainland, increasing pollutant concentrations. The episode examined belongs to the ESCOMPTE pre-campaign (available at

June 29, 2000



June 30, 2000

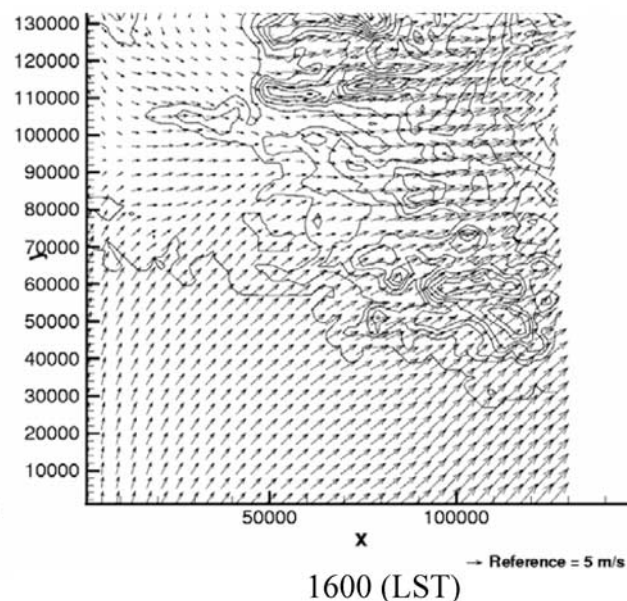
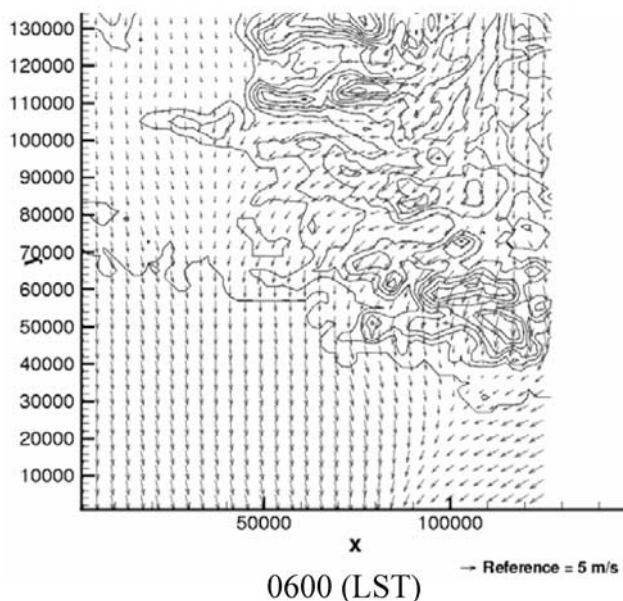


Figure 6. Wind fields ~ 10 m above ground level for the GMA episode of June 29 and June 30, 2000 at 0600 LST and 1600 LST.

<http://medias.obs-mip.fr/escompte>). However, during the ESCOMPTE campaign the sea breeze circulation was documented at the South France [Bastin *et al.*, 2003]. The Rhone and Durance valleys at Marseille area can modify the wind flow, but their influence differs since they don't have the same orientation and width. Moreover, the Durance valley transports pollutants inland, which may be incorporated into long-range transport since the depth of the breeze flow increases.

[43] The predicted concentrations of SO_4^- , NO_3^- , NH_4^+ , OC at two representative monitoring stations in Marseille and Toulon without biogenic emissions, as well as the increase

due to the presence of biogenic gasses are also presented in Figure 9. After midday, there is an increase in the concentrations of ozone and aerosol species for both days of the simulation, due to the increased photochemical activity. The time series of NH_4^+ concentration followed that of SO_4^- . SO_4^- is the most abundant ionic compound in the stations presented, indicative of the strong photochemical production of sulfate in the city center. This is the result of transport of increased SO_2 concentrations from the industrial areas, which in turn form H_2SO_4 . The predicted results when biogenic emissions are included confirm that they alter the concentrations of inorganic aerosol species

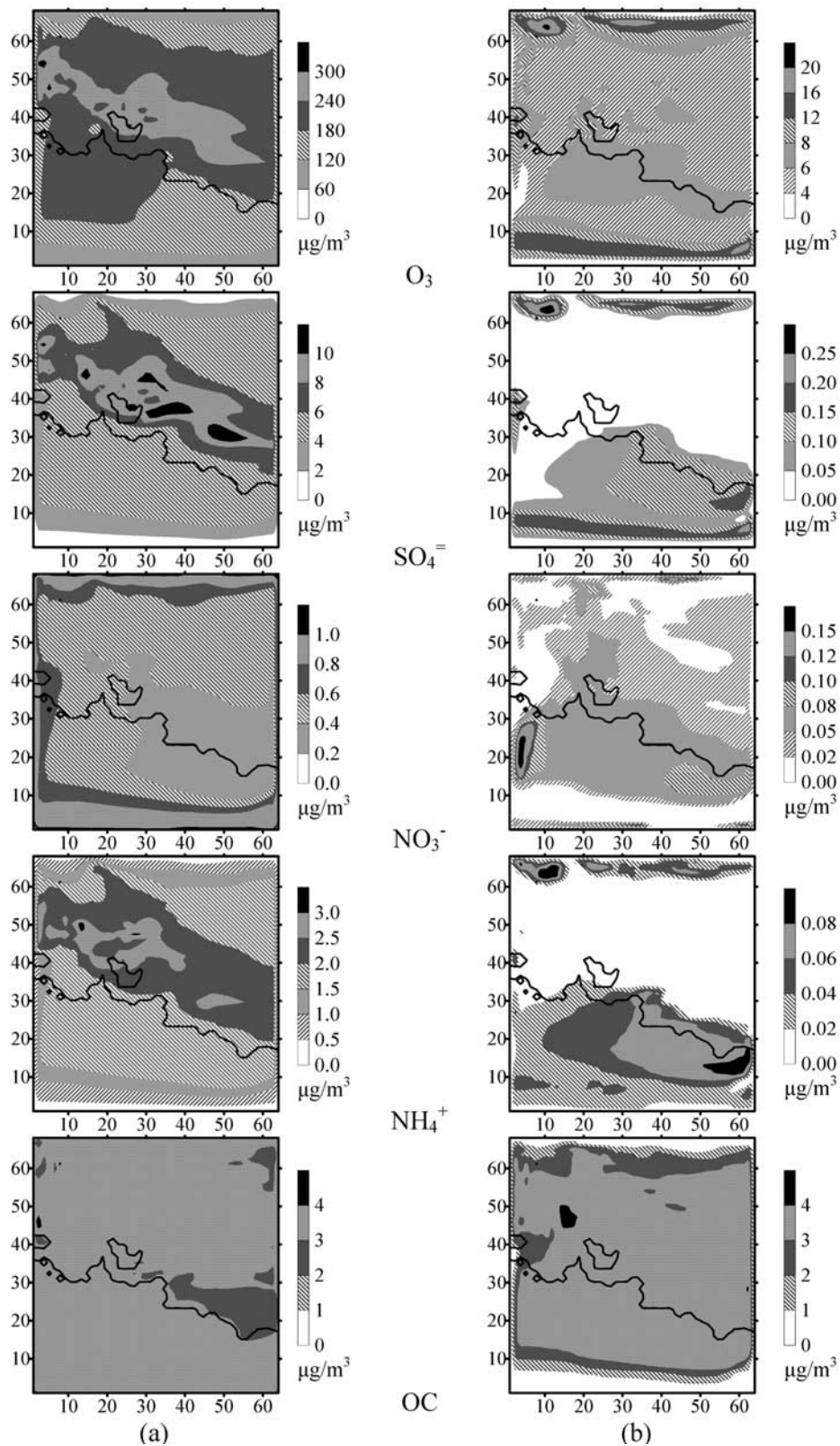


Figure 7. Spatial distributions of (a) predicted ground level concentrations in the GMA at 1800 LST when no biogenic emissions are used, and (b) predicted increase in the corresponding concentrations when biogenic emissions are included. See color version of this figure in the HTML.

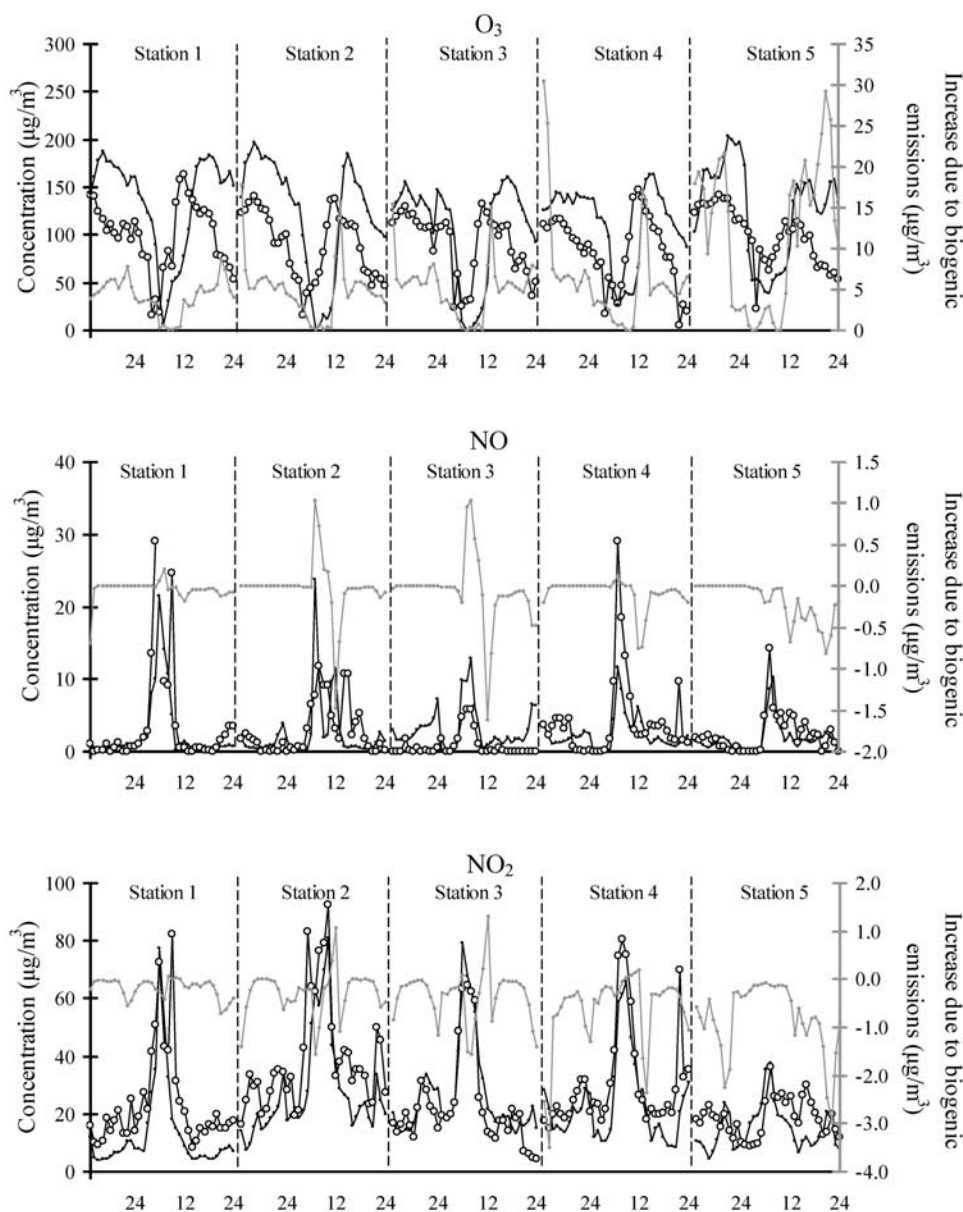


Figure 8. Predicted (squares) and observed (circles) time series concentrations (left y-axes) and increase (diamonds) due to biogenic emissions (right y-axes) for five monitoring stations in the GMA. See color version of this figure in the HTML.

through the production of OH from the ozonolysis of terpenes. This reaction is responsible for the decrease of O_3 concentrations and the increase of inorganic aerosol species during the morning hours. Moreover, the modeling results showed, as in the case of Athens, that the maximum percent impact of biogenic emissions on ozone and aerosol concentrations does not coincide in time with their maximum concentrations.

3.3. Comparison of the Results for Greater Athens Area and Greater Marseilles Area

[44] Comparing the predicted concentrations for the two areas of interest, it is noticeable that O_3 and secondary PM concentrations are influenced by biogenic emissions in both areas. However, this influence is more profound in the city of Marseilles than in the city of Athens, due to the wind

field and the higher biogenic emissions in GMA. Terpene emissions are ~ 300 kmol/day for GAA, while for GMA are 400 kmol/day. The respective isoprene emissions are 130 kmol/day for GAA and 1720 kmol/day for GMA. So, the maximum 1-h average O_3 concentration when biogenic emissions are included is 5% higher for the city-center of Athens and 25% higher for the city-center of Marseilles. The reaction of the substantially higher terpenes in GMA, compared to those in GAA, with gaseous NO_3 , OH radicals and O_3 form larger OC quantities. In a similar fashion, the higher OH radicals formed by the ozonolysis of terpenes in GMA, compared to GAA, leads to the formation of higher quantities H_2SO_4 and HNO_3 due to its reactions with SO_2 and NO_x , respectively. These two acids condensate to form aerosol sulfates and nitrates. So, the 24-h average concentrations of secondary PM_{2.5} are

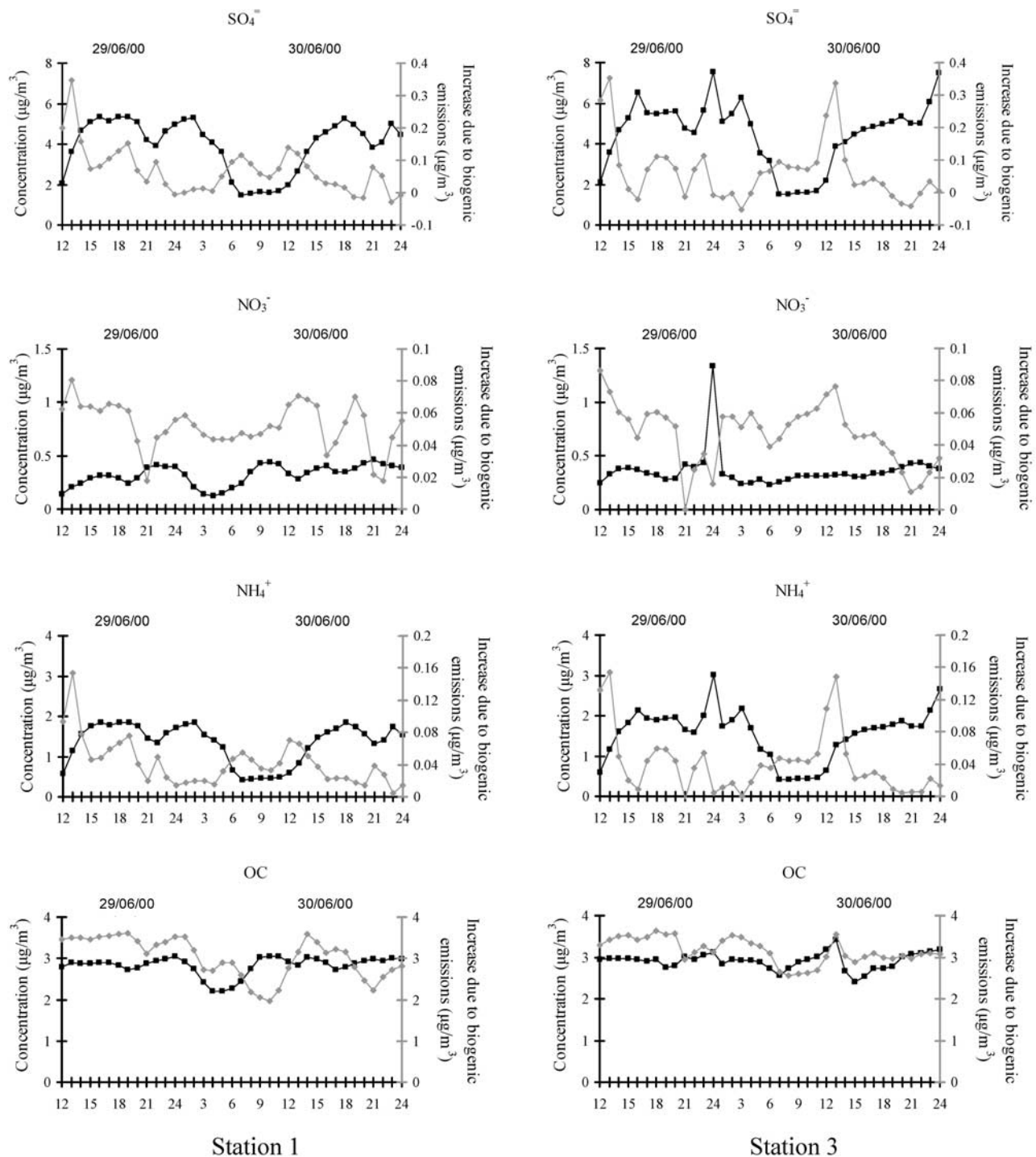


Figure 9. Predicted (squares) time series concentrations (left y-axes) and increase (diamonds) due to biogenic emissions (right y-axes) for two monitoring stations in the GMA.

increased by 2% in the Athens city-center and 29% in the city-center of Marseilles with the inclusion of biogenic emissions, while the respective percentages for secondary PM10 are 1% and 17%. The smaller predicted increase in secondary PM10 concentrations compared to secondary PM2.5 is due to fact that the median diameter of the main secondary aerosols is smaller than $2.5 \mu\text{m}$ [Seinfeld and Pandis, 1998]. In a similar study performed in the Eastern

United States [Pun *et al.*, 2002] it was reported that the contribution of biogenic emissions to 1-h average O_3 concentrations in urban locations was 22–34%, while the contribution to secondary PM2.5 24-h average concentrations was 4–13%. Although it is not correct to compare estimates of the contribution of biogenic emissions on both ozone and secondary PM concentrations in urban areas, as they depend on the prevailing wind fields and the magni-

Table 1. Impact of Biogenic Emissions on Ozone and Aerosol Concentrations for Different Scenarios

Scenarios	O ₃ (μg/m ³)					Secondary PM10 (μg/m ³)				
	ST 1	ST 2	ST 3	ST 4	ST 5	ST 1	ST 2	ST 3	ST 4	ST 5
Estimation with the existing data	8.7	17.8	15.5	30.5	29.2	3.9	4.2	4.1	4.7	3.9
NO 30% emissions increase	9.0	23.7	25.0	39.7	32.4	3.9	4.3	4.4	4.9	4.0
HC 30% emissions increase	8.7	20.6	21.0	36.2	29.0	3.9	4.2	4.3	4.7	3.8
20% wind increase in x-direction	8.6	16.8	18.4	34.7	29.4	3.8	4.0	4.0	4.7	3.9
20% wind increase in y-direction	9.8	20.0	17.1	31.2	24.4	3.6	4.0	3.8	4.6	3.8
0.7*HV	9.5	16.3	14.0	27.5	26.0	3.9	4.0	4.1	4.8	4.3

tude of biogenic emissions in the area of interest, their results are in a qualitative agreement with ours.

3.4. Sensitivity Analysis

[45] There are uncertainties associated with this kind of exercises, i.e., application of a 3-D model in order to determine the impact of a parameter, which in our case is the contribution of biogenic emissions to ozone and aerosol species concentrations. These include uncertainties in the inputs, like the emission inventories and the meteorological conditions, and uncertainties due to the parameterization of the model, like due to the chemical mechanism, for example. It is crucial to examine whether the results of the simulations are sensitive to the input data. To do so, we performed a sensitivity analysis of the model for GMA, as there the contribution of biogenic emissions to the concentrations of ozone and aerosol species is more significant than for GAA. The scenarios considered include a thirty percent (30%) increase of NO emissions, thirty percent (30%) increase of all emitted hydrocarbons, twenty percent (20%) increase of the velocity of the wind in the x-direction, twenty percent (20%) increase of the velocity of the wind in the y-direction and finally one run during which the solar radiation is adapted to the seventy percent (70%) of the solar radiation (HV) used in the original run. As in the original application of the model, in order to avoid any domination of the initial conditions onto the predictions, multiple repeated runs were performed. In each scenario we applied the model twice, one without biogenic emissions and another one with biogenic emissions. For these two runs of each scenario, the predicted concentrations for ozone and aerosol species are intercompared, in order to determine the contribution of biogenic emissions. Table 1 shows the maximum impact of biogenic emissions during the period of the simulation (in μg/m³) for the five stations for which we have presented results. The results are those of all the scenarios along with the results of the original application, i.e., with the existing emission inventory and wind field for the days of simulation.

[46] It is noticeable in Table 1 that the impact of biogenic emissions on ozone is more sensitive than the impact on aerosol concentrations to uncertainties in the input. Some stations show higher sensitivity than others. We can conclude though that there is a significant contribution of biogenic emissions on both ozone and aerosol despite uncertainties.

4. Conclusions

[47] The ADREA-I/UAM-AERO modeling system was applied in two air pollution episodes, one in Athens, Greece and one in Marseilles, France. For each episode two simulations were performed, a base case without biogenic emissions and a case with biogenic emissions. Com-

parison of the results reveals the significant role biogenic emissions play in the formation aerosol species. Although the model was applied for two different locations with different topography, anthropogenic and biogenic emissions, as well as under different meteorological fields, the influence of biogenic emissions was significant in aerosol formation, as well as in ozone concentrations in both areas. The importance, however, is more profound in GMA due to the wind field and the higher amount of biogenic emissions.

[48] An increase in the maximum 1-hour average ozone concentration up to 5% in the Athens city-center and 25% in the city-center of Marseilles is estimated when biogenic emissions are considered. The model also predicts that aerosol concentrations will increase in both city-centers. In Athens, the concentration of secondary PM2.5 is 2% higher due to biogenic gasses while the secondary PM10 is 1% higher. The effect is more profound for Marseilles with values of 29% and 17% for secondary PM2.5 and PM10, respectively. So, under the examined weather conditions, biogenic emissions influence more the Marseilles air quality than Athens.

[49] The results of this study show that, not only the concentrations of OC are affected, but also the concentrations of the inorganic aerosol species, due to the production of OH from the reaction of terpenes with ozone. The modeling results also showed that the maximum percent impact of biogenic emissions on both ozone and aerosol concentrations do not coincide in time with their maximum concentrations.

[50] Despite the role biogenic emissions play, they should not be considered responsible for atmospheric pollution episodes. Anthropogenic emissions are the main causes of high levels of atmospheric pollution in urban areas. Biogenic emissions, though, should be taken under consideration when models for the prediction, as well as for the enforcement of abatement strategies of atmospheric pollution are applied, even if biogenic sources are placed mostly in the countryside. Taking into consideration the shown importance of species of biogenic origin, further research is necessary, in order to improve the biogenic chemistry that is used by the models, as well as to refine biogenic emission inventories.

[51] **Acknowledgments.** This study is part of the project Biogenic Aerosols and Air Quality in the Mediterranean Area and is supported by EU through grant EVK2-CT-2001-00107 (BOND) of Directorate D16. The authors would like to thank Phillip Mirabel for providing the data for the GMA and the two reviewers for their very constructive suggestions.

References

- Andreae, M. O., and P. J. Crutzen (1997), Atmospheric aerosols: Biogeochemical sources and role in atmospheric chemistry, *Science*, 276, 1052–1058.
- Andronopoulos, S., J. G. Bartzis, P. Kalabokas, and A. Passamichali (1998), Computational Simulation of a Photochemical Air-Pollution Episode in Athens, *Fresenius Environ. Bull.*, 7, 299–306.

- Atkinson, R. (2000), Atmospheric chemistry of VOCs and NOx, *Atmos. Environ.*, *34*, 2063–2101.
- Atkinson, R., and J. Arey (1998), Atmospheric chemistry of biogenic organic compounds, *Account. Chem. Res.*, *31*, 574–583.
- Bartziis, J. G. (1989), Turbulent diffusion modelling for wind flow and dispersion analysis, *Atmos. Environ.*, *23*, 1963–1969.
- Bartziis, J. G., A. Venetsanos, M. Varvayanni, N. Catsaros, and A. Megaritou (1991), ADREA-I: A transient three-dimensional transport code for complex terrain and other applications, *Nucl. Technol.*, *94*, 135–148.
- Bastin, S., et al. (19–23 May 2003), Impact of complex terrain on sea-breeze circulation during ESCOMPTE IOP2b, paper presented at ICAM/MAP Conference, MeteoSwiss, Brig, Switzerland.
- Cabada, J. C., S. N. Pandis, and A. L. Robinson (2002), Sources of atmospheric carbonaceous particulate matter in Pittsburg, Pennsylvania, *J. Air Waste Manage. Assoc.*, *52*, 732–741.
- Carter, W. P. L. (1990), A detailed mechanism for the gas-phase atmospheric reactions of organic compounds, *Atmos. Environ.*, *3*, 481–518.
- Chameides, W. L., R. W. Lindsay, J. Richardson, and C. S. Kiang (1988), The role of biogenic hydrocarbons in urban photochemical smog: Atlanta as a case study, *Science*, *241*, 1473–1475.
- Geron, C., R. Rasmussen, R. R. Arnts, and A. Guenther (2000), A review and synthesis of monoterpene speciation from forests in the United States, *Atmos. Environ.*, *34*, 1761–1781.
- Geron, C., P. Harley, and A. Guenther (2001), Isoprene emission capacity for US tree species, *Atmos. Environ.*, *35*, 3341–3352.
- Geron, C., A. Guenther, J. Greenberg, H. W. Loesch, D. Clark, and B. Baker (2002), Biogenic volatile organic compound emissions from lowland tropical wet forest in Costa Rica, *Atmos. Environ.*, *36*, 3793–3802.
- Glasius, M., M. Lahaniati, A. Calogirou, D. Di Bella, N. R. Jensen, J. Hjorth, D. Kotzias, and B. R. Larsen (2000), Carboxylic acids in secondary aerosols from oxidation of cyclic monoterpenes by ozone, *Environ. Sci. Technol.*, *34*, 1001–1010.
- Greenberg, J. P., A. Guenther, P. Zimmermann, W. Baugh, C. Geron, K. Davis, D. Helmig, and L. F. Klinger (1999), Tethered balloon measurements of biogenic VOCs in the atmospheric boundary layer, *Atmos. Environ.*, *33*, 855–867.
- Griffin, R. J., D. Dabdub, and J. H. Seinfeld (2002), Secondary organic aerosol I. Atmospheric chemical mechanism for production of molecular constituents, *J. Geophys. Res.*, *107*(D17), 4332, doi:10.1029/2001JD000541.
- Grosjean, D., and J. Seinfeld (1989), Parameterization of the formation potential of secondary organic aerosols, *Atmos. Environ.*, *23*, 1733–1747.
- Guenther, A., C. Geron, T. Pierce, B. Lamb, P. Harley, and R. Fall (2000), Natural emissions of non-methane volatile organic compounds, carbon monoxide, and oxides of nitrogen from North America, *Atmos. Environ.*, *34*, 2005–2230.
- Helmig, D., L. F. Klinger, A. Guenther, L. Vierling, C. Geron, and P. Zimmermann (1999a), Biogenic volatile organic compound emissions (BVOCs) I. Identifications from three continental sites in the U.S., *Chemosphere*, *38*, 2163–2187.
- Helmig, D., L. F. Klinger, A. Guenther, L. Vierling, C. Geron, and P. Zimmermann (1999b), Biogenic volatile organic compound emissions (BVOCs) II. Landscape flux potentials from three continental sites in the U.S., *Chemosphere*, *38*, 2189–2204.
- Hindmarsh, A. C. (1983), ODEPACK: A systematized collection of ODE solvers, in *Scientific Computing*, edited by R. S. Stepleman et al., pp. 55–64, North-Holland, New York.
- Hoffmann, T., J. Odum, F. Bowman, D. Collins, D. Klockow, R. C. Flagan, and J. H. Seinfeld (1996), Aerosol formation potential of biogenic hydrocarbons, *J. Aerosol Sci.*, *27*, S233–S234.
- Hoffmann, T., J. Odum, F. Bowman, D. Collins, D. Klockow, R. C. Flagan, and J. H. Seinfeld (1997), Formation of organic aerosols from the oxidation of biogenic hydrocarbons, *J. Atmos. Chem.*, *26*, 189–222.
- Isebrands, J. G., A. B. Guenther, P. Harley, D. Helmig, L. Klinger, L. Vierling, P. Zimmermann, and C. Geron (1999), Volatile organic compound emission rates from mixed deciduous and coniferous forests in Northern Wisconsin, USA, *Atmos. Environ.*, *33*, 2527–2536.
- Jacobson, M. C., H. C. Hansson, K. J. Noone, and R. J. Charlson (2000), Organic atmospheric aerosols: Review and state of the science, *Rev. Geophys.*, *38*, 267–294.
- Jang, M., and R. M. Kamens (1999), Newly characterized products and composition of secondary aerosols from the reaction of α -pinene with ozone, *Atmos. Environ.*, *33*, 459–474.
- Koch, S., R. Winterhalter, E. Uherek, A. Koloff, P. Neeb, and C. K. Moortgat (2000), Formation of new particles in the gas-phase ozonolysis of monoterpenes, *Atmos. Environ.*, *34*, 4031–4042.
- Kotroni, V., G. Kallos, K. Lagouvardos, M. Varinou, and R. Walko (1999), Numerical Solutions of the Meteorological and Dispersion Conditions during an Air Pollution Episode over Athens, Greece, *J. Appl. Meteorol.*, *38*, 432–447.
- Kulmala, M., et al. (2001), Overview of the international project on biogenic aerosol formation in the boreal forest (BIOFOR), *Tellus, Ser. B*, *53*, 324–343.
- Kumar, N., F. W. Lurmann, and W. P. L. Carter (1995), Development of the flexible chemical mechanism version of the urban airshed model (STI-94470-1508-FR), Sonoma Technology, Inc., Santa Rosa, Calif.
- Nenes, A., C. Pilinis, and S. N. Pandis (1998), ISORROPIA: A new thermodynamic model for inorganic multicomponent atmospheric aerosols, *Aquat. Geochem.*, *4*, 123–152.
- Nenes, A., S. N. Pandis, and C. Pilinis (1999), Continued development and testing of a new thermodynamic aerosol module for urban and regional air quality models, *Atmos. Environ.*, *33*, 1553–1560.
- Nowak, D. J., K. L. Civerolo, R. S. Tsvikrama, G. Sistla, C. J. Luley, and D. E. Crane (2000), A modelling study of the impact of urban trees on ozone, *Atmos. Environ.*, *34*, 1601–1613.
- Pandis, S. N., R. A. Harley, G. R. Cass, and J. H. Seinfeld (1992), Secondary organic aerosol formation and transport, *Atmos. Environ.*, *26A*, 2269–2282.
- Pfeiffer, T., O. Forberich, and F. J. Comes (1998), Tropospheric OH formation by ozonolysis of terpenes, *Chem. Phys. Lett.*, *298*, 351–358.
- Pierce, T. E., B. K. Lamb, and A. R. Van Meter (1990), Development of a biogenic emissions inventory system for regional scale air pollution models, paper presented at 83rd Annual Meeting, Air and Waste Manage. Assoc., Pittsburgh, Penn.
- Pilinis, C., P. Kassomenos, and G. Kallos (1993), Modeling of photochemical pollution in Athens, Greece. Application of the RAMS-CALGRID modeling system, *Atmos. Environ.*, *4*, 353–370.
- Poisson, N., et al. (2001), The impact of natural non-methane hydrocarbon oxidation on the free radical and ozone budgets above an eucalyptus forest, *Chemosphere*, *3*, 353–366.
- Pun, B. K., S. Y. Wu, and C. Seigneur (2002), Contribution of biogenic emissions to the formation of ozone and particulate matter in the Eastern United States, *Environ. Sci. Technol.*, *36*, 3586–3596.
- Seinfeld, J., and S. N. Pandis (1998), *Atmospheric Chemistry and Physics*, John Wiley, Hoboken, N. J.
- Simpson, D., et al. (1999), Inventorying emissions from nature in Europe, *J. Geophys. Res.*, *104*, 8113–8152.
- Sonoma Technology, Inc. (1996), User's guide to the UAM-AERO model, *STI-93110-1600-UG*, Peteluma, Calif.
- Sotiropoulou, R. E. P., and C. Pilinis (2001), Modeling of photochemical pollution in Athens, Greece: Application of the UAM-AERO and CALGRID modeling systems, in *Proceedings of the 7th International Conference of Environmental Science Technoogy.*, pp. 813–820, Univ. of the Aegean, Ermoupolis, Syros Island, Greece.
- Sotiropoulou, R. E. P., E. Tagaris, and C. Pilinis (2004), An estimation of the spatial distribution of agricultural ammonia emissions in the Greater Athens Area, *Sci. Total Environ.*, *318*, 159–169.
- System Applications International (SAI) (1990a), User's guide for the urban airshed model, vol. 1, *Rep. SYSAPP-90/018a*, San Rafael, Calif.
- System Applications International (SAI) (1990b), User's guide for the urban airshed model, vol. 1, *Rep. SYSAPP-90/018b*, San Rafael, Calif.
- System Applications International (SAI) (1990c), User's guide for the urban airshed model, vol. 1, *Rep. SYSAPP-90/018c*, San Rafael, Calif.
- System Applications International (SAI) (1990d), User's guide for the urban airshed model, vol. 1, *Rep. SYSAPP-90/018d*, San Rafael, Calif.
- System Applications International (SAI) (1990e), User's guide for the urban airshed model, vol. 1, *Rep. SYSAPP-90/018e*, San Rafael, Calif.
- Thunis, P., and C. Cuvelier (2000), Impact of biogenic emissions on ozone formation in the Mediterranean area: A BEMA modelling study, *Atmos. Environ.*, *34*, 467–481.
- Varinou, M., G. Kallos, G. Tsiligriridis, and G. Sistla (1999), The role of anthropogenic and biogenic emissions on Tropospheric ozone formation over Greece, *Phys. Chem. Earth, Part C*, *24*, 507–513.
- Varvayannis, M., J. G. Bartziis, N. Catsaros, P. Deligiannis, and C. E. Elderkin (1997), Simulation of nocturnal drainage flows enhanced by deep canyons: The Rocky Flats case, *J. Appl. Meteorol.*, *36*, 775–791.
- Wesely, M. L. (1989), Parameterization of surface resistances to gaseous dry deposition in regional-scale numerical models, *Atmos. Environ.*, *23*, 1293–1304.
- Yu, J., D. R. Cocker, R. J. Griffin, R. C. Flagan, and J. H. Seinfeld (1999), Gas-phase ozone oxidation of monoterpenes: Gaseous and Particulate products, *J. Atmos. Chem.*, *34*, 207–258.

S. Andronopoulos, J. G. Bartziis, and A. Sfetsos, Environmental Research Laboratory, NCSR Demokritos, GR-15310 Aghia Paraskevi, Attiki, Greece.
C. Pilinis, R. E. P. Sotiropoulou, and E. Tagaris, Department of Environmental Studies, University of the Aegean, University Hill, GR-81100 Mytilene, Lesvos, Greece. (xpil@aegean.gr)